Supplementary Material

for

Modeling Microplastic Transport from Watersheds to Estuaries with a Coupled Hydrologic–Estuarine Framework

Zhuoran Duan Yicheng Huang Mark Wigmosta Zhi Li Ning Sun
Taiping Wang Zhaoqing Yang Ben Maurer

1 Microplastics Size Distribution Parameterization

To map literature microplastics size distributions onto the 0.1–100μm airborne MP range of the [1] dataset, we propose a generalized parameterization that integrates trends for sizes smaller and larger than 100 μm. [2] reports that for particles larger than 20 μm the size distribution scales as $\sim s^{-1.6}$, implying that occurrence density decreases with increasing size in that regime. In contrast, airborne source data from [1] show that for particles smaller than 10 μm the distribution scales as $\sim s^{1.4}$, meaning the occurrence density decreases with decreasing size. To merge these two behaviors continuously, To merge these two behaviors continuously, we define:

$$x^* = \ln x, \quad x \text{ in } \mu\text{m},$$

and adopt the following generalized probability density function:

$$f(x) = A \exp\left[(\beta_1 + \beta_2)x^* - \beta_2 x_0^* + \beta_2 \ln\left(1 + e^{-(x^* - x_0^*)}\right) - \beta_2\right]. \tag{S1}$$

This form recovers the empirical scalings in the limits:

- For $x \ll x_0$ (i.e., $s \ll e^{x_0}$): $f(x) \propto e^{\beta_1 x} \sim s^{\beta_1}$,
- For $x \gg x_0$ (i.e., $s \gg e^{x_0}$): $f(x) \propto e^{(\beta_1+\beta_2)x} \sim s^{\beta_1+\beta_2}$,

so that the small-size and large-size asymptotic exponents are $\beta_1 \approx 1.42$ and $\beta_1 + \beta_2 \approx -1.6$, respectively. The fitted parameter values are

$$A = 0.0016, \quad \beta_1 = 1.42, \quad \beta_2 = -3.02, \quad x_0^* = \ln x_0 = \ln 15. \tag{S2}$$

Figure S1 shows the distribution from Equation S1 over the full MP size range 0.1 μm to 5×10^3 μm). The proposed form captures the asymptotic behavior at both the small- and large-size limits while exhibiting a mode near $x \approx 15$ μm.

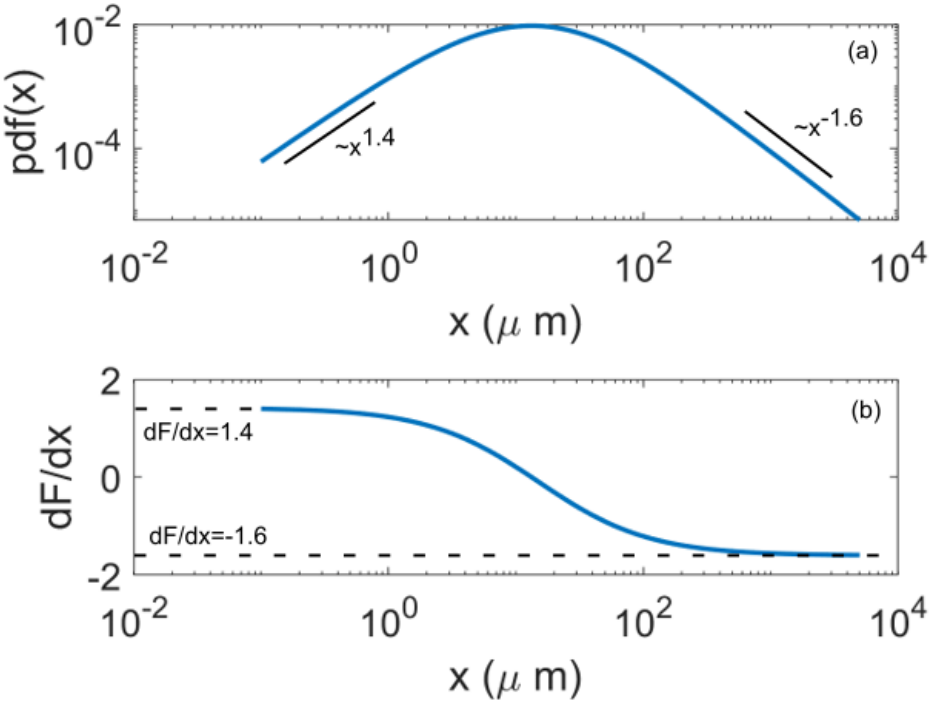

Figure S1: Probability distribution of MP. (a) size distribution pdf diagram; (b) size distribution asymptotes.

2 Waste-Water-Treatment-Plant Microplastics Concentration Parameterization

To estimate MP concentrations in wastewater treatment plant (WWTP) effluent, we extended the MP effluent concentration dataset from [3] and compiled a global dataset comprising 269 effluent MP measurements reported in 50 studies. The geographic (continental) coverage of the source studies is shown in Figure S2(a), and the individual data contributions are summarized in Figure S2(c). Observed MP number concentrations span from 3.2 to 1.78×10^6 $\#/m^3$ (Figure S2b); the corresponding quantiles are listed in Table S1. Using Equation S1, the MP size distribution in the effluent is rescaled to the range 0.1 μm–100 μm, resulting in a centroid size of $r_c = 39.84$ μm, which serves as the characteristic particle size. For the model, the number concentration C^{number} is converted to a mass concentration C^{mass} by assuming each particle is a sphere of uniform density. The mass of a single particle is

$$m = \frac{4}{3}\pi\rho r_c^3,$$

so the conversion is

$$c^{\text{mass}} = c^{\text{number}} \times \left(\frac{4}{3}\pi\rho r_c^3\right). \tag{S3}$$

Here ρ is the MP density, assumed to be 1 g/cm^3 (consistent with [1]). Number concentrations at each quantile are converted to mass concentrations via Equation S3; the results are reported in Table S1. The dataset is supplied as the supplementary spreadsheet 'WWTP-supplementary.xlsx'.

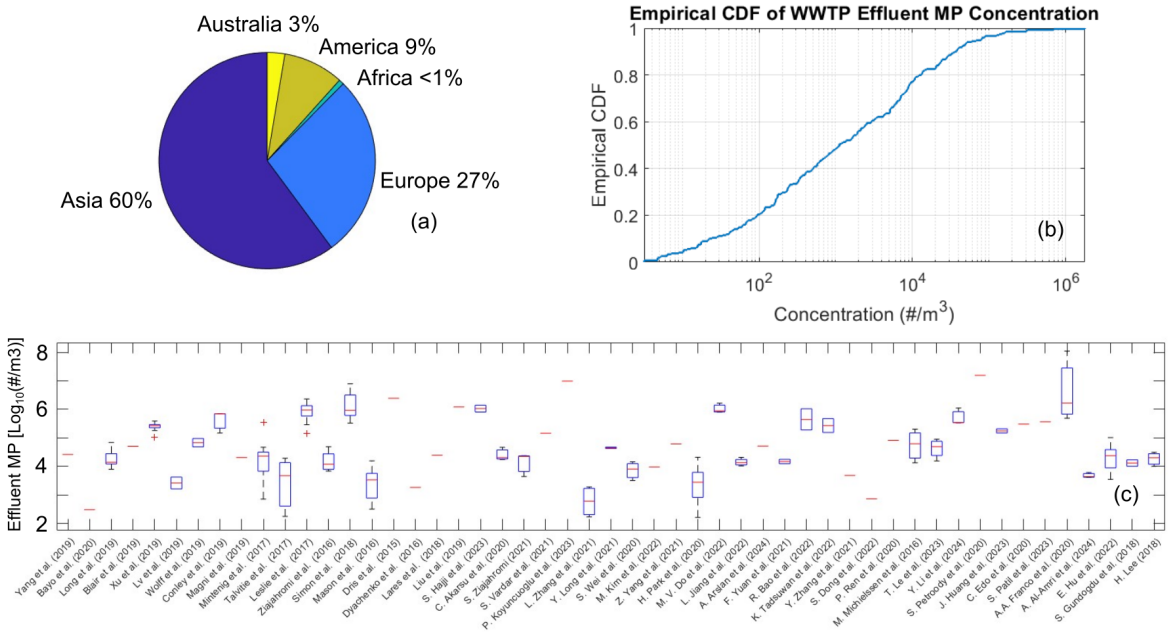

Figure S2: Meta-analysis and summary statistics of microplastic (MP) concentrations in WWTP effluent. (a) Geographic distribution of effluent measurements by continent. (b) Distribution of MP concentrations across all samples. (c) Boxplot summarizing the range and variability of MP concentrations from all included studies.

Table S1: Summary statistics for microplastic concentrations in the 0.1–100 μm size range.

Statistic	Number concentration c^{number} (#/m^3)	Mass concentration c^{mass} (g/m^3)
Min	3.20×10^{0}	8.47×10^{-7}
25% quantile	1.60×10^{2}	4.22×10^{-5}
50% quantile	1.12×10^{3}	2.95×10^{-4}
75% quantile	8.88×10^{3}	2.35×10^{-3}
Max	1.78×10^{6}	4.72×10^{-1}

3 Wash-off Model Configuration

The wash-off process is driven by runoff Q, which is derived from precipitation intensity P through a rational conversion that accounts for land-type specific infiltration and threshold behavior. This relationship is written as:

$$Q = \max\{0, C\,(P - f)\}, \tag{S4}$$

where C is the runoff coefficient for the given land type and f is the threshold representing that land type's permeability or initial resistance to generating runoff (see Table S2). By definition, $Q = 0$ when $P \leq f$.

Two wash-off formulations are implemented in our model framework. In addition to the linear wash-off model (equation 2 in main text) used in the case study, we also include the exponential wash-off model that has been applied in the Storm Water Management Model (SWMM) and in several other studies [4–7] and which informed our parameter selection. In the exponential formulation, the fractional wash-off increases nonlinearly with runoff, combining the initiation threshold with a saturating response:

$$F_{\text{wash-off}}^{\text{exp}} = 1 - \exp(-K_w Q). \tag{S5}$$

Here, Q is the runoff, and K_w is the wash-off coefficient controlling how rapidly the wash-off fraction approaches unity as Q increases. Typical values of K_w vary by surface type; the range used here, based on common calibration values for SWMM implication, is 0.039 to 0.39 mm^{-1}, spanning from highly pervious to fully impervious land covers [8]. Figure S3 and Figure S4 illustrate three representative land types, including the pervious and impervious extremes. We also examine the response using a default value $K_w = 0.18$ mm^{-1} adopted in SWMM [1, 7], which represents a typical mixed urban land cover; its wash-off behavior is shown in Figure S3 (variation with runoff) and Figure S4 (variation with precipitation). For comparison, the equivalent linear wash-off model corresponding to each exponential scenario is also shown in Figure S3 and Figure S4. The equivalent linear model is defined by choosing its slope so that it attains 98% of the exponential model's asymptotic wash-off at the same runoff level.

Because direct measurements of the movability threshold are not available, we infer its configuration from indirect observations of microplastic (MP) mobilization following rainfall events and from prior modeling studies. In [1], a very low threshold of $R_c = 2$ mm/day was used. Another study [9] found that rainfall exceeding 40 mm/week (i.e., > 5.7 mm/day) led to enhanced stormwater runoff capable of transporting additional MPs from surrounding catchments, substantially increasing local MP concentrations in stormwater ponds. A separate work [10] identified a pronounced first-flush effect at precipitation rates of 38 mm/day. Guided by these findings, the movability threshold in the present work is set below 38 mm/day. For each land type we present three initialization thresholds: zero adhesion ($R_c = 0$), medium adhesion ($R_c = 16$ mm/day), and high adhesion ($R_c = 32$ mm/day). With the transferring using rational method by S4, the initialization run-off threshold q_{low}^t can be obtained. The case for different adhesion scenario represented by run-off or precipitation are shown at Figure S3 and Figure S4.

From the nine scenarios shown in Figures S3 and S4, one intermediate case is selected to represent a typical microplastic wash-off parameterization for the present study (see Figure S3e and S4).

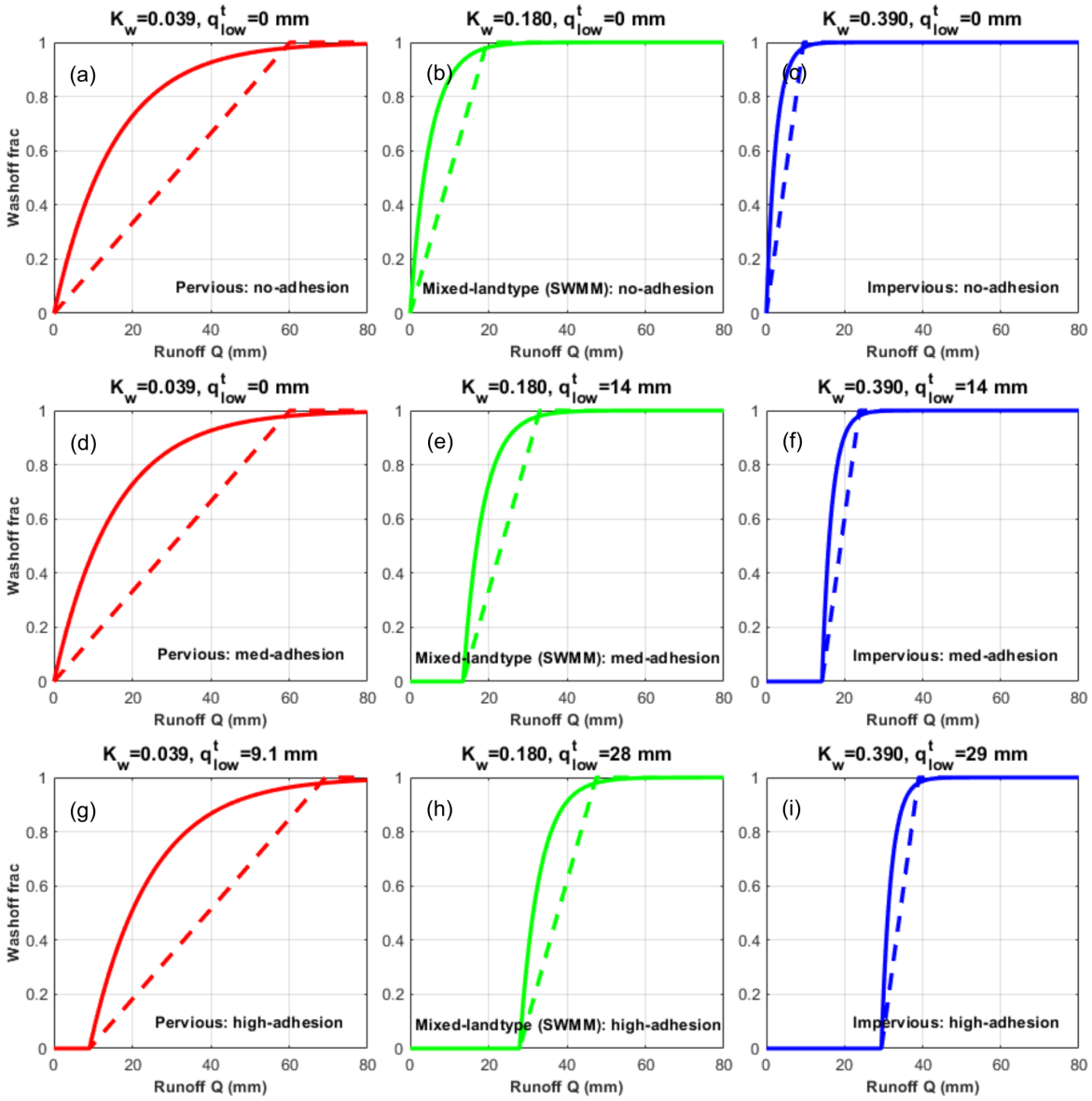

Figure S3: Wash-off function as a function of run-off strength (mm/day) for linear (dash-line) and exponential model at different initialtion threshold and land-type set-up.

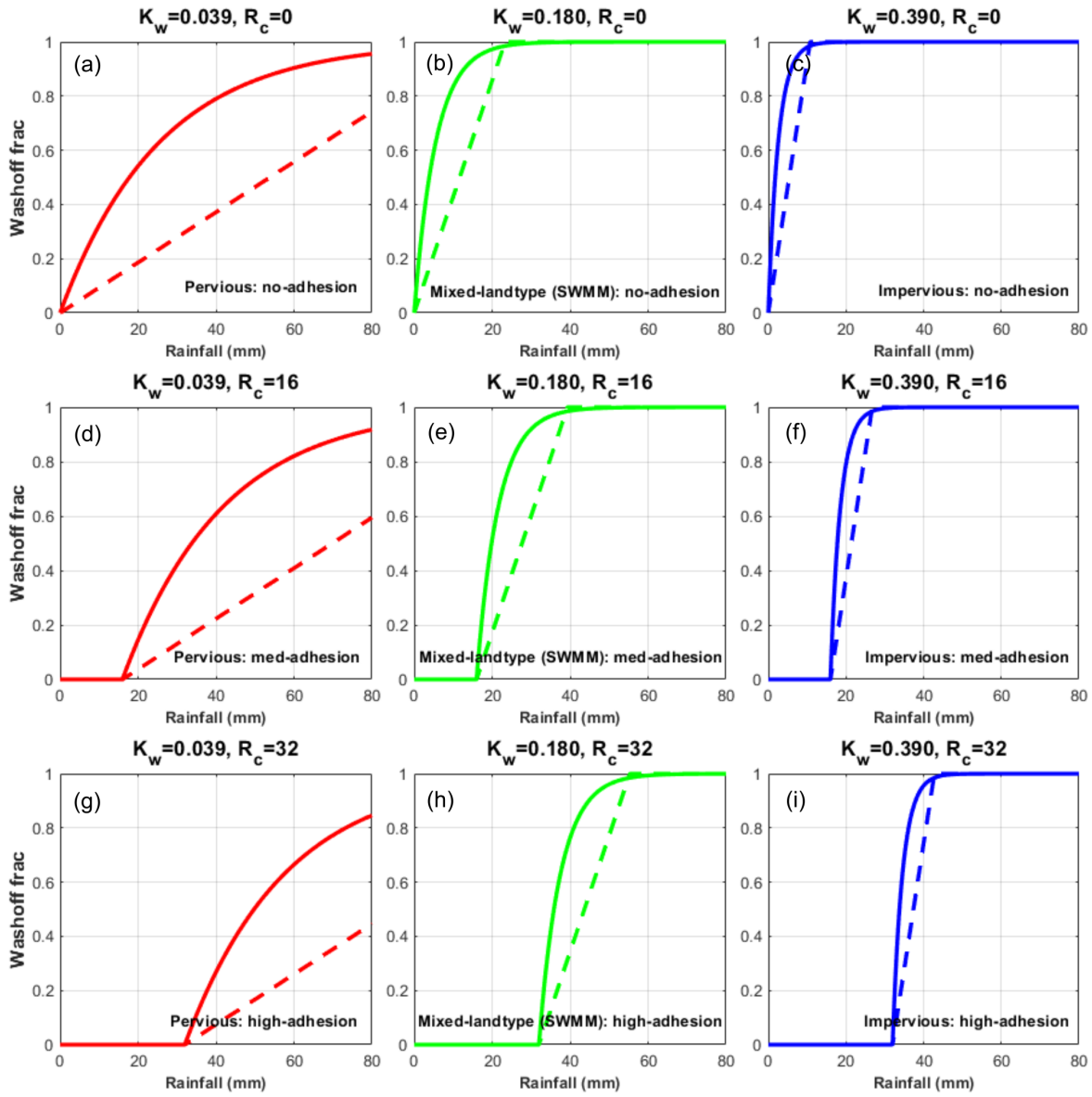

Figure S4: Wash-off function as a function of precipitation strength (mm/day) for linear (dash-line) and exponential model at different initialtion threshold and land-type set-up.

Table S2: Wash-off parameters for different land types.

Land-type	C	f (mm)	K_w (1/mm)	k (1/mm)
Pervious (empirical limit)	0.6	16.9	0.039	0.022
Mixed	0.9	1.0	0.18	0.067
Impervious (empirical limit)	0.95	1.0	0.39	0.14

4 DHSVM discharge outlet

For the standalone DHSVM cases, the estuarine discharge boundary is specified as the sum of all upstream discharge volumes from the sub-watersheds within the Delaware River Basin, released through a single outlet at the mouth of the Delaware River. The configured stream network is shown in Figure S5, with the Delaware River outlet at the river mouth highlighted.

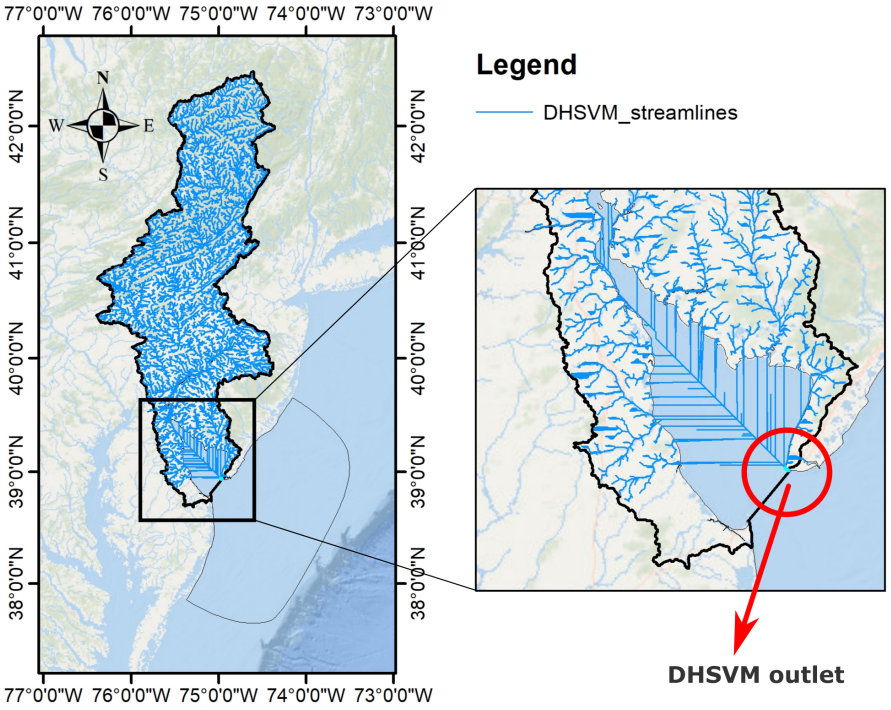

Figure S5: Stream network configuration for DHSVM, and the discharge port set-up at the Delaware River mouth.

References

[1] KM Unice, MP Weeber, MM Abramson, RCD Reid, JAG Van Gils, AA Markus, AD Vethaak, and JM Panko. "Characterizing export of land-based microplastics to the estuary-Part I: Application of integrated geospatial microplastic transport models to assess tire and road wear particles in the Seine watershed". In: *Science of the total environment* 646 (2019), pp. 1639–1649.

[2] Merel Kooi and Albert A Koelmans. "Simplifying microplastic via continuous probability distributions for size, shape, and density". In: *Environmental Science & Technology Letters* 6.9 (2019), pp. 551–557.

[3] Christian Schmidt, Rohini Kumar, Soohyun Yang, and Olaf Büttner. "Microplastic particle emission from wastewater treatment plant effluents into river networks in Germany: Loads, spatial patterns of concentrations and potential toxicity". In: *Science of the Total Environment* 737 (2020), p. 139544.

[4] Xi Luo, Xuyong Li, Jingqiu Chen, Qingyu Feng, Yunjie Liao, Manli Gong, and Junyu Qi. "Modeling urban pollutant wash-off processes with ecological memory". In: *Journal of Environmental Management* 373 (2025), p. 123786.

[5] Mohammed N Assaf, Sauro Manenti, Enrico Creaco, Carlo Giudicianni, Lorenzo Tamellini, and Sara Todeschini. "New optimization strategies for SWMM modeling of stormwater quality applications in urban area". In: *Journal of Environmental Management* 361 (2024), p. 121244.

[6] Veljko Prodanovic, Behzad Jamali, Martijn Kuller, Yanni Wang, Peter Marcus Bach, Rhys A Coleman, Leon Metzeling, David T McCarthy, Baiqian Shi, and Ana Deletic. "Calibration and sensitivity analysis of a novel water flow and pollution model for future city planning: Future Urban Stormwater Simulation (FUSS)". In: *Water Science and Technology* 85.4 (2022), pp. 961–969.

[7] Lewis A Rossman et al. *Storm water management model user's manual, version 5.0*. Vol. 276. National Risk Management Research Laboratory, Office of Research and ..., 2010.

[8] U.S. Army Corps of Engineers, Hydrologic Engineering Center. *Build-up Wash-off*. HEC-HMS Technical Reference Manual. Accessed August 4, 2025. 2025. URL: https://www.hec.usace.army.mil/confluence/hmsdocs/hmstrm/erosion-and-sediment-transport-under-construction/erosion-methods/build-up-wash-off.

[9] Wan Nadiah Amalina Kadir, Bojan Tamburic, Chung Yiin Wong, Richard M Stuetz, and Andrew P Dansie. "Comparative and temporal analysis of microplastic abundance and type in urban stormwater catchments". In: *Environmental Challenges* (2025), p. 101216.

[10] Youna Cho, Won Joon Shim, Sung Yong Ha, Gi Myung Han, Mi Jang, and Sang Hee Hong. "Microplastic emission characteristics of stormwater runoff in an urban area: Intra-event variability and influencing factors". In: *Science of the Total Environment* 866 (2023), p. 161318.